

# NO-REFERENCE BLUR ASSESSMENT IN NATURAL IMAGES USING FOURIER TRANSFORM AND SPATIAL PYRAMIDS

*Eftichia Mavridaki, Vasileios Mezaris*

Information Technologies Institute / CERTH, Thessaloniki 57001, Greece  
{emavridaki, bmezaris}@iti.gr

## ABSTRACT

In this paper we propose a no-reference image blur assessment model that performs partial blur detection in the frequency domain. Specifically, our method exploits the information derived from the power spectrum of the Fourier transform. The latter is computed for both the entire image and several patches of it, in order to estimate the distribution of low and high frequencies, and is appropriately encoded so as to preserve some information about the spatial arrangement of the frequency distribution in the image. Finally, a Support Vector Machine (SVM) classifier is applied to the above features, serving as the image blur quality evaluator. For a proper training and evaluation of the proposed method, we proceeded with creating and using a large image dataset consisting of more than 2400 digital photographs, which we make publicly available. The results show the efficiency of our method in assessing not only artificially-distorted images but also naturally-blurred ones.

**Index Terms**— No-Reference image blur assessment, blur detection, Fourier transform, Support Vector Machine.

## 1. INTRODUCTION

Blur is one of the most commonly encountered image distortion types in digital photos, since it can be caused during the capturing of an image (e.g., out-of-focus, motion blur, etc.), as well as during image manipulation procedures such as image compression. Blur detection techniques aim to quantify the amount of blur in digital images and classify them as blurred or non-blurred according to their visual quality. In this way, the distorted images can be detected and removed or even possibly restored, leading to the enhancement of multimedia preservation in terms of media quality and required storage space. Therefore, the development of image blur assessment techniques, particularly techniques that will effectively deal with naturally-blurred images, is an appealing field of research.

The proposed method aims to achieve partial blur assessment using the frequency power spectrum of both the entire image and individual parts of it. The rest of this paper is organized as follows. In section 2 we review the related work. In section 3 we present the proposed approach in detail. In section 4 the datasets and the experimental results are discussed and finally, conclusions are drawn in section 5.

## 2. RELATED WORK

In recent years, a variety of image blur assessment methods have been proposed in the relevant literature and many of them are based

---

This work was supported by the European Commission under contracts FP7-600826 ForgetIT and FP7-287911 LinkedTV.



**Fig. 1:** Two image examples: (a) a well-focused (yet partially-blurred) image, (b) a blurred (out-of-focus) image.

on edge detection. For instance, the authors of [1] propose a local blur measure for the estimation of the presence of blur on each pixel along the image's edges. The method of [2] exploits the local edges gradient to provide a sharpness metric. The average extent of the edges is also used to quantify the blur degradation in [3], while in [4] blur detection is based on the evaluation of the ratio and the mean value of a quantity defined as "edge blurriness". The blur metric proposed in [5] is also based on edge detection, specifically on evaluating the average edge width. A more elaborate method is proposed in [6], where the notion of Just Noticeable Blur (JNB) is introduced for expressing the presence of blur around an edge. Based on the idea of JNB, the authors of [7] compute the Cumulative Probability of Blur Detection (CPBD) at the image edges to quantify the image sharpness. Edge-based blur quantification methods are often susceptible not only to the general problems of threshold selection at the edge detection step, but also to the presence of noise, as discussed in [8].

To avoid performing edge detection, several other classes of blur assessment methods have appeared in the literature. For instance, in the method presented in [9] the presence of blur is estimated by quantifying the difference between the variations of neighbouring pixels before and after a low pass filtering step. In [10] and [11] the image distortion quantification is achieved by employing Natural Scene Statistics (NSS), in the spatial and in the frequency domain respectively, as well as a supervised learning approach. The authors of [12] also tried to assess image blurring using a combination of NSS, multi-resolution decomposition methods and machine learning techniques.

All the above techniques detect the presence of blur distortion and assess the visual quality by looking at the overall image, without taking into account that an image can be partially-blurred. A partially-blurred image can still have high aesthetic quality, as can be seen from the photo shown in Fig. 1(a). In [13], a partial blur detection approach is proposed which exploits the information of several image features, including saturation, contrast, gradient, end others, extracted from image patches.

In the relevant literature, there are also many transform-

frequency-based methods. In [14], a no-reference sharpness measure based on the local edge kurtosis of the DCT coefficients is proposed, while in [15] a histogram-based measure exploits the distribution of non-zero DCT coefficients to perform blur detection. The authors of [16] assess the image sharpness as the Local Phase Coherence (LPC) of the wavelet image coefficients. In [17], a blur detection approach is proposed which exploits the Haar wavelet transform and sets a threshold value to quantify the edge sharpness level.

Methods based on the Fourier transform include [18]-[24]. In [18] and [19] the authors estimate the sum of the power spectra coefficients to characterize the image sharpness, while in [20] the amplitude spectrum slope is employed. Moreover, in [21], the authors propose an SVM-based learning system in order to predict the parameters that determine the motion and the out-of-focus blur. In [22], sharpness evaluation is performed by exploiting both spectral and spatial image information. The method proposed in [23] takes advantage of frequency domain analysis using image patch information for training an SVM classifier to track motion-blurred targets in a video. In [24], a review on motion blur detection is presented where several frequency-based techniques are discussed. Although the above methods are related to the present study, our method demonstrates a new, simple yet effective technique to perform frequency domain analysis and encode its results for blur detection in still images, which to our knowledge has not appeared in the relevant literature. Furthermore, the above frequency-based still image assessment methods do not take into account information about the spatial arrangement of the Fourier transform outputs; spatial information has however been shown to provide significant advantages in other image analysis tasks, such as visual concept detection, e.g. spatial pyramids proposed in [25].

Specifically, the present work attempts to quantify the impact of blurring on the perceived image quality and aesthetics by examining not only the entire image, but also individual parts of it. For this, we propose a frequency domain scheme which exploits the information of the frequency spectrum and appropriately represents it with some form of spatial pyramids so as to also preserve spatial information about the frequency distribution. We then use this in combination with a supervised learning model to estimate the blur degradation and determine whether a given image is blurred or not without introducing the need for heuristically selecting any threshold values.

### 3. PROPOSED BLUR DETECTION SCHEME

#### 3.1. Basic principle

During the process of image capture, the image may undergo several degradations. One of them is blurring, which occurs when a low-pass filter is applied on the image. In the real world, blurring may be caused by the opening and closing speed of the shutter, atmospheric turbulence, out-of-focus of the lens, or relative motion between the camera, a moving object and the background. In most of the above cases, the result is the attenuation of high frequencies, which affects the frequency spectrum of the image. The proposed blur detection approach exploits this fundamental principle and attempts to analyse the image in the frequency domain using the Fourier transform.

The process of blurring can be described by the following convolution equation,

$$g(x, y) = i(x, y) * h(x, y) + n(x, y) \quad (1)$$

where,  $i(x, y)$  is the original image,  $h(x, y)$  is the blurring Point-Spread Function (PSF),  $n(x, y)$  is additive noise and  $g(x, y)$  is the

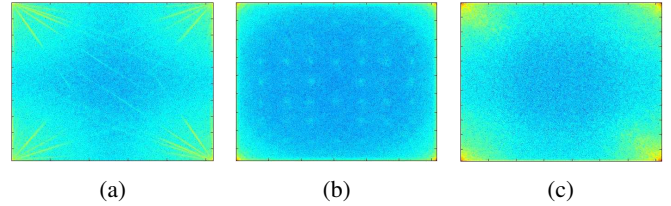


**Fig. 2:** Power spectrum examples: (a) undistorted image, (b) artificially-blurred image, (c) naturally-blurred image. Higher density regions indicate the low power of high frequencies.

degraded image. The Fourier transform of the degraded image can be represented by the following model,

$$G(u, v) = I(u, v) \cdot H(u, v) + N(u, v) \quad (2)$$

where  $G(u, v)$ ,  $I(u, v)$ ,  $H(u, v)$  and  $N(u, v)$  are the Fourier transform of  $g(x, y)$ ,  $i(x, y)$ ,  $h(x, y)$  and  $n(x, y)$ , respectively. In the proposed method, we exploit the information derived from the power spectrum of the Fourier transform, which is estimated by the following equation,

$$Power = 10 \cdot (|G|^2 + 1) \quad (3)$$

As shown in Fig. 2, the power spectra of an undistorted, an artificially-blurred and a naturally-blurred image have significant differences. Therefore, the main goal is to effectively capture the proper information of the power spectrum in order to classify an image as blurred or not. Below, we present a new, efficient technique to identify the high-frequencies distribution of the image power spectrum.

#### 3.2. Partial blur image assessment, an aesthetic approach

Photographs that have one specific, well-focused point of interest are usually more appealing to the viewers. Professional photographers often focus on the subject of interest, intentionally leaving the background out of focus. Consequently, there are high quality photos that are well-focused on a particular subject while exhibiting partial out-of-focus blur, as shown in Fig. 1(a). This kind of images may mislead the majority of blur detection methods that examine the presence of blur on the image as a whole.

To prevent such quality assessment errors, we adopt a partial blur detection scheme. This involves exploiting spatial pyramids, and in particular partitioning the original image into 9 equal blocks according to the rule of thirds [26] and taking into account the power spectra of both the entire image and each of the 9 aforementioned patches for assessing the presence of blur. Thus, even in the case of partially-blurred images we can correctly identify them as such. We chose the aforementioned 9 patches based on preliminary experiments which demonstrated that smaller patches are not able to properly describe the blur degradation, while larger patches fail to sufficiently capture the partial blur.

Specifically, our method takes an image as an input, which is then partitioned into 9 patches. Subsequently, the power spectrum is computed accordingly to Eq. (3), not only for the entire image, but also for each of its 9 patches separately. Therefore, 10 different power spectra are estimated for the input image. Then, the challenge is to quantify the contained high frequencies. We refrain from setting a threshold value that would be applied to the outcome of Eq. (3) at this point, since this would be an ad-hoc solution making our system sensitive to input data variability. Instead, we estimate a 5-bin

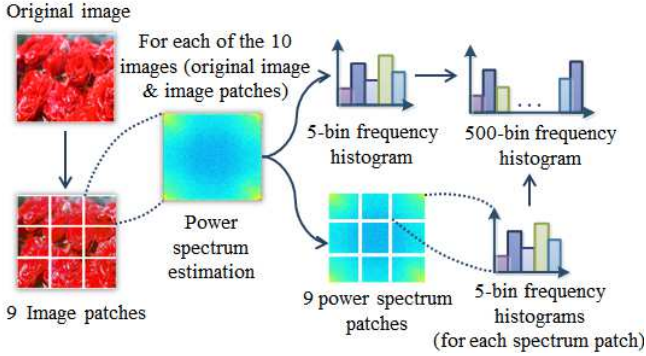


Fig. 3: Overview of our partial blur detection method

frequency histogram for each of the power spectra, by subdividing the frequency amplitude according to the following ranges:  $[0, 100]$ ,  $[100, 150]$ ,  $[150, 200]$ ,  $[200, 300]$  and  $[300, max]$ . These ranges were experimentally found to be suitable for our application. In addition, for greater spatial accuracy, we further divide each of the ten power spectra into 9 equal patches (Fig. 3) and compute such histograms for each spectrum patch. Finally, all calculated 5-bin histograms are concatenated in a 500-element vector, which following normalization of its elements in the range  $[0, 1]$  serves as the input to an SVM classifier [27]. After applying the trained SVM classifier to an input image, a confidence value is obtained, indicating the probability that this image is blurred. The overall procedure of the proposed blur detection method is presented in Fig. 3 and in Algorithm 1.

---

#### Algorithm 1 Partial Blur Detection

---

**Input:** An image  $I$ .

**Output:** A blur confidence value.

- 1: Convert the RGB image  $I(x,y,3)$  into gray level image  $I_1(x,y)$ .
  - 2: Partition  $I_1(x,y)$  into equal 9 parts,  $I_p(x,y)$ , where  $p = 2, \dots, 10$ .
  - 3: Compute the Fourier transform  $I_p(u,v)$  according to Eq. (2), where  $p = 1, 2, \dots, 10$ .
  - 4: Compute the power spectrum  $PS_p(u,v)$  according to Eq. (3), where  $p = 1, 2, \dots, 10$ .
  - 5: **for**  $p = 1 : 10$  **do**
  - 6:   Estimate the 5-bin frequency histogram of the  $PS_p(u,v)$
  - 7:   Partition the  $PS_p(u,v)$  into equal 9 patches,  $PS_{patch_{pi}}$
  - 8:   **for**  $i = 1 : 9$  **do**
  - 9:     Estimate the 5-bin frequency histogram of the  $PS_{patch_{pi}}$
  - 10:   **end for**
  - 11: **end for**
  - 12: Evaluation of the  $1 \times 500$  input vector by the trained SVM classifier.
- 

## 4. EXPERIMENTAL RESULTS AND DISCUSSION

### 4.1. Datasets and Evaluation

Most image blur assessment approaches have been tested on publicly available image datasets, e.g. [28] and [29], which provide the reference (undistorted) images together with artificially-blurred variations of them. In the present work, we aim to perform blur detection not only on artificially-distorted images, which are globally blurred with low-pass filters, but also on real photos, where any blur distortion has been caused by external conditions and detecting it

is much more challenging. For this reason, we created a large image dataset consisting of 2450 digital images with the corresponding ground-truth which indicates whether each image is blurred or not. The ground-truth was generated by human inspection of the images.

In our dataset, 1850 of the images are photos captured by various camera models in different shooting conditions that have not been altered in any way following their capture, while the remaining 600 are artificially-blurred images. Out of the 1850 non-altered photos, 1219 are clear, undistorted images (70 of them exhibit intentional partial blur), while the remaining 631 are blurred images, exhibiting mostly out-of-focus and motion blur. For the creation of the 600 artificially-distorted images, 60 of the aforementioned undistorted images were randomly chosen and then several types of Gaussian, motion and circular averaging filters were applied to them in order to simulate different levels of degradation, similarly to [9] (see<sup>1</sup> for details on the applied filters). The resolution of the images in our dataset ranges from  $960 \times 1280$  to  $4000 \times 2248$  pixels. The image dataset and the ground-truth image quality assessments that are introduced in this section have been made publicly available<sup>1</sup>.

As mentioned above, our method uses an SVM classifier to assess whether an image is degraded by blur or not. For training this SVM classifier, we used 630 undistorted (28 of them are partially-blurred), 220 naturally-blurred and 150 artificially-distorted images chosen from the aforementioned CERTH image blur dataset and 40 of the undistorted images, resized to  $384 \times 512$  and  $512 \times 512$  pixels. The selection of the  $C$  and the  $\gamma$  parameters of the SVM was performed using a ten-fold cross validation on this training set. Subsequently, the remaining 1450 images of the CERTH image blur dataset were used for evaluation, divided into two sets: the ‘‘Natural Blur’’ testset, which contains 411 naturally-blurred and 589 undistorted images, and the ‘‘Artificial Blur’’ testset, which contains 450 artificially-blurred and 30 undistorted images derived from the ‘‘Natural Blur’’ testset. In both cases, besides the training and the evaluation sets being disjoint, we made sure that the majority of images used for the evaluation were taken by different cameras than those used for the training.

Finally, the performance of our blur detection approach is evaluated calculating the overall Accuracy, Precision, Recall and F-score values,

$$Accuracy = \frac{TP + TN}{\#I} \quad Precision = \frac{TP}{TP + FP}$$

$$Recall = \frac{TP}{\#B}$$

where,  $TP$  (True Positives) is the number of blurred images correctly identified as blurred,  $FP$  (False Positives) is the number of undistorted images incorrectly identified as blurred,  $TN$  (True Negatives) is the number of undistorted images correctly identified as undistorted,  $\#I$  is the total number of images and  $\#B$  is the total number of blurred images in the testset. F-score is also calculated as the harmonic mean of Precision and Recall.

### 4.2. Results and Discussion

We use both the ‘‘Natural Blur’’ and the ‘‘Artificial Blur’’ evaluation set in order to test our method’s performance and compare with previously proposed methods for which the corresponding code has been released. Specifically, we compare with the Blind Image Quality Index (BIQI) [11] and the Blind / Referenceless Image Spatial Quality Evaluator (BRISQUE) [10], which, similarly to

<sup>1</sup>The CERTH image blur dataset, <http://mklab.itl.gr/project/imageblur>

**Table 1:** Experimental results on CERTH testsets

“Natural Blur” testset										
Metrics	Proposed method	CDLN [9]	BIQI [11]	BIQI blur [11]	BRISQUE [10]	JNB [6]	CPBD [7]	LPC [16]	S3 [22]	MDWE [5]
FP	62	366	298	145	280	164	243	134	114	133
FN	66	134	149	108	91	160	208	114	107	147
Accuracy	<b>0.8720</b>	0.5000	0.5530	0.7470	0.6290	0.6760	0.5490	0.7520	0.7790	0.7200
Precision	<b>0.8394</b>	0.4308	0.4679	0.6763	0.5333	0.6048	0.4552	0.6891	0.7273	0.6650
Recall	<b>0.8394</b>	0.6740	0.6375	0.7372	0.7786	0.6107	0.4939	0.7226	0.7397	0.6422
F-score	<b>0.8394</b>	0.5256	0.5396	0.7055	0.6330	0.6077	0.4737	0.7055	0.7334	0.6535
Run Time	23min	35min	25min	25min	35min	294min	270min	294min	~38h	38min
“Digital Blur” testset										
Metrics	Proposed method	CDLN [9]	BIQI [11]	BIQI blur [11]	BRISQUE [10]	JNB [6]	CPBD [7]	LPC [16]	S3 [22]	MDWE [5]
FP	0	15	23	9	11	10	8	6	5	8
FN	4	7	5	16	2	74	40	18	2	13
Accuracy	<b>0.9917</b>	0.9542	0.9417	0.9479	0.9729	0.8250	0.9000	0.9500	0.9854	0.9563
Precision	<b>1</b>	0.9672	0.9509	0.9797	0.9760	0.9741	0.9809	0.9886	0.9890	0.9820
Recall	0.9911	0.9844	0.9889	0.9644	<b>0.9956</b>	0.8356	0.9111	0.9600	<b>0.9956</b>	0.9711
F-score	<b>0.9955</b>	0.9758	0.9695	0.9720	0.9857	0.8995	0.9447	0.9741	0.9922	0.9765
Run Time	8min	12min	9.5min	9.5min	11min	109min	80.5min	114min	~20h	45min

our approach, are learning based methods, and the following non-learning-based methods: the blur metric from Crete *et al.* (CDLN) [9], the JNB algorithm [6], the CPBD algorithm [7], the LPC-based algorithm [16], the spatial and spectral algorithm S3 [22] and the perceptual blur metric from Marziliano *et al.* (MDWE) [5]. The first two methods are used for image quality assessment in general, but also examine the blur distortion. In addition, BIQI provides a specific model for blur detection (BIQI blur), which we also examine separately. For all these methods we used the parameter values specified by the authors in the corresponding papers. It should be noted that all the above methods produce a score in a pre-specified range (e.g. [0, 1]) to indicate the level of blur that is detected, rather than making a binary decision. In order to calculate the evaluation measures of section 4.1, we transformed the scores into binary blur / non-blur decisions by searching the most appropriate threshold value for each method separately, for the given image collections. The results of the performance evaluation and comparisons are shown in Table 1. As can be seen, all examined methods achieve high performance for artificially-distorted images, but the results on naturally-blurred images do not always remain similarly high. On the challenging and realistic problem of detecting natural blur, the proposed method achieves the best results, followed by the S3 algorithm and the LPC-based method. In comparison to the latter, the proposed method exhibits a relative improvement of 12%-22% in terms of Accuracy, Precision, Recall and F-score.

The BIQI and BRISQUE methods were originally trained on a small dataset [28], which consisted of approximately 200 artificially degraded images for the blur distortion. In order to assess the impact of their training on the results, we re-trained them using the

same CERTH training dataset that we used for the training of the proposed approach, again computing the proper  $C$ ,  $\gamma$  and  $\epsilon$  using ten-fold cross validation. After the re-training, the BIQI achieves Accuracy = 0.78 and F-score = 0.74, while BRISQUE achieves Accuracy = 0.78 and F-score = 0.75 on the “Natural Blur” testset. From these results it is evident that the proposed approach still significantly outperforms the BIQI and BRISQUE methods in detecting naturally-blurred images, even after their more extensive training.

Having presented the experimental results of our blur detection method on the CERTH image dataset, we now test it on the TID artificially-blurred dataset [29], and on the BID naturally-blurred dataset [30], to further demonstrate its good performance. The results are shown in Table 2, where we can see that our method achieves high performance on these datasets, which is also consistently higher than the performance of the other methods that we compare with (again, after the re-training of the BIQI and BRISQUE algorithms using our extensive training set).

In addition, it is worth noting that our blur detection method correctly classified 75 out of the 90 partially-blurred images that exist in the BID dataset and 36 out of the 42 partially-blurred images that exist in the “Natural Blur” testset of the CERTH image blur dataset.

At this point, we should mention that our experiments aimed to evaluate not only the Accuracy of these methods but also their execution time, as this plays a crucial role in real-time applications. All the experiments were performed on an Intel Core i7 PC (3.50 GHz, 16 GB RAM, Windows 7 64-bit). The corresponding results are summarized in Table 1, where we can see that our approach has low computational complexity as it needs 23 minutes for processing a collection of 1000 images of size ranging from 960x1280 to 4000x2248 pixels (i.e. approximately 1.4 sec. per image). This is similar to or less than the processing time of the other methods of Table 1.

**Table 2:** Experimental results on TID and BID dataset

Metrics	Accuracy		F-score	
	TID	BID	TID	BID
Proposed method	<b>0.96</b>	<b>0.81</b>	<b>0.98</b>	<b>0.80</b>
CDLN [9]	0.84	0.54	0.91	0.57
BIQI blur [11]	0.93	0.75	0.96	0.73
BRISQUE [10]	0.91	0.69	0.94	0.66
JNB [6]	0.92	0.61	0.96	0.49
CPBD [7]	0.80	0.58	0.86	0.56
LPC [16]	0.95	0.70	0.96	0.67
S3 [22]	<b>0.96</b>	0.76	0.97	0.71
MDWE [5]	0.89	0.72	0.93	0.71

## 5. CONCLUSION

In this paper, we proposed a new image partial blur assessment approach, working on the frequency domain, which analyses the high- and low-frequency distribution of the power spectra and uses a supervised machine learning method. This approach results in a non-reference blur detection model which, as shown by the experimental results, presents promising performance in real-time blur assessment for both artificially- and naturally-blurred images.

## 6. REFERENCES

- [1] G. Cao, Y. Zhao, and R. Ni, "Edge-based blur metric for tamper detection," *Journal of Information Hiding and Multimedia Signal Processing*, vol. 1, no. 1, pp. 20–27, 2010.
- [2] C. Feichtenhofer, H. Fassold, and P. Schallauer, "A perceptual image sharpness metric based on local edge gradient analysis," *Signal Processing Letters, IEEE*, vol. 20, no. 4, 2013.
- [3] E. P. Ong, W. Lin, Z. Lu, X. Yang, S. Yao, F. Pan, L. Jiang, and F. Moschetti, "A no-reference quality metric for measuring image blur," in *Proc. of Seventh International Symposium on Signal Processing and Its Applications*, vol. 1, pp. 469–472, 2003.
- [4] M. Choi, J. Jung, and J. Jeon, "No-reference image quality assessment using blur and noise," in *Proc. of World Academy of Science, Engineering and Technology*, vol. 38, pp. 163–167, 2009.
- [5] P. Marziliano, F. Dufaux, S. Winkler, and T. Ebrahimi, "A no-reference perceptual blur metric," in *Proc. of IEEE Int. Conf. on Image Processing*, vol. 3, pp. III–57, 2002.
- [6] R. Ferzli and L. J. Karam, "A no-reference objective image sharpness metric based on the notion of just noticeable blur (jnb)," *IEEE Transactions on Image Processing*, vol. 18, no. 4, pp. 717–728, 2009.
- [7] N. D. Narvekar and L. J. Karam, "A no-reference image blur metric based on the cumulative probability of blur detection (cpbd)," *IEEE Transactions on Image Processing*, vol. 20, no. 9, pp. 2678–2683, 2011.
- [8] E. Nadernejad, S. Sharifzadeh, and H. Hassanpour, "Edge detection techniques: evaluations and comparisons," *Applied Mathematical Sciences*, vol. 2, no. 31, pp. 1507–1520, 2008.
- [9] F. Crete, T. Dolmiere, P. Ladret, and M. Nicolas, "The blur effect: perception and estimation with a new no-reference perceptual blur metric," *Human vision and electronic imaging XII*, vol. 6492, pp. 64920I, 2007.
- [10] A. Mittal, A. K. Moorthy, and A. C. Bovik, "No-reference image quality assessment in the spatial domain," *IEEE Transactions on Image Processing*, vol. 21, pp. 4695–4708, 2012.
- [11] A. K. Moorthy and A. C. Bovik, "A two-step framework for constructing blind image quality indices," *Signal Processing Letters, IEEE*, vol. 17, no. 5, pp. 513–516, 2010.
- [12] M. J. Chen and A. C. Bovik, "No-reference image blur assessment using multiscale gradient," *Journal on Image and Video Processing, EURASIP*, vol. 2011, no. 1, pp. 1–11, 2011.
- [13] R. Liu, Z. Li, and J. Jia, "Image partial blur detection and classification," in *Proc. of IEEE Conf. on Computer Vision and Pattern Recognition (CVPR'08)*, pp. 1–8, 2008.
- [14] J. Cavedes and F. Oberti, "A new sharpness metric based on local kurtosis, edge and energy information," *Signal Processing: Image Communication*, vol. 19, no. 2, pp. 147–161, 2004.
- [15] X. Marichal, W. Y. Ma, and H. J. Zhang, "Blur determination in the compressed domain using dct information," in *Proc. of ICIP Int. Conf. on Image Processing, IEEE*, vol. 2, pp. 386–390, 1999.
- [16] R. Hassen, Z. Wang, and M. Salama, "Image sharpness assessment based on local phase coherence," *IEEE Transactions on Image Processing*, vol. 22, no. 7, 2013.
- [17] H. Tong, M. Li, H. Zhang, and C. Zhang, "Blur detection for digital images using wavelet transform," in *Proc. of IEEE Int. Conf. on Multimedia and Expo (ICME'04)*, vol. 1, pp. 17–20, 2004.
- [18] L. Firestone, K. Cook, K. Culp, N. Talsania, and K. Preston, "Comparison of autofocus methods for automated microscopy," *Cytometry*, vol. 12, no. 3, pp. 195–206, 1991.
- [19] N. B. Nill and B. Bouzas, "Objective image quality measure derived from digital image power spectra," *Optical engineering*, vol. 31, no. 4, pp. 813–825, 1992.
- [20] D. J. Field and N. Brady, "Visual sensitivity, blur and the sources of variability in the amplitude spectra of natural scenes," *Vision research*, vol. 37, no. 23, pp. 3367–3383, 1997.
- [21] R. Dash, P. K. Sa, B. Majhi, et al., "Blur parameter identification using support vector machine," *International Journal on Control System and Instrumentation, ACEEE*, vol. 3, no. 2, 2012.
- [22] C. T. Vu, T. D. Phan, and D. M. Chandler, "S3: A spectral and spatial measure of local perceived sharpness in natural images," *IEEE Transactions on Image Processing*, vol. 21, no. 3, pp. 934–945, 2012.
- [23] S. Dai, M. Yang, Y. Wu, and A. K. Katsaggelos, "Tracking motion-blurred targets in video," in *Proc. of IEEE Int. Conf. on Image Processing*, pp. 2389–2392, 2006.
- [24] S. Tiwari, V. P. Shukla, and A. K. Singh, "Certain investigations on motion blur detection and estimation," in *Proc. of Int. Conf. on Signal, Image and Video Processing, IIT Patna*, pp. 108–114, 2012.
- [25] S. Lazebnik, C. Schmid, and J. Ponce, "Beyond bags of features: Spatial pyramid matching for recognizing natural scene categories," in *IEEE Computer Society Conference on Computer Vision and Pattern Recognition*, vol. 2, pp. 2169–2178, 2006.
- [26] L. Mai, H. Le, Y. Niu, and F. Liu, "Rule of thirds detection from photograph," in *Proc. of IEEE International Symposium on Multimedia (ISM)*, pp. 91–96, 2011.
- [27] C. C. Chang and C. J. Lin, "Libsvm: a library for support vector machines," *ACM Transactions on Intelligent Systems and Technology (TIST)*, vol. 2, no. 3, pp. 27, 2011.
- [28] H. R. Sheikh, Z. Wang, L. Cormack, and A. C. Bovik, "Live image quality assessment database release 2," <http://live.ece.utexas.edu/research/quality/>, 2007.
- [29] N. Ponomarenko, V. Lukin, A. Zelensky, K. Egiazarian, M. Carli, and F. Battisti, "Tid2008-a database for evaluation of full-reference visual quality assessment metrics," *Advances of Modern Radioelectronics*, vol. 10, no. 4, pp. 30–45, 2009.
- [30] E. A. B. da Silva, "Bid-real blurred image database," <http://www.lps.ufrj.br/profs/eduardo/ImageDatabase.htm>, 2013.